Evaluation of the AWAP daily precipitation spatial analysis with an independent gauge network in the Snowy Mountains

Thomas H. Chubb,[1,2] Michael J. Manton,[1] Steven T. Siems,[1,3] and Andrew D. Peace[2]

[1] School of Earth, Atmosphere, and Environment; Monash University, Victoria, Australia
[2] Snowy Hydro Ltd.; Sydney, New South Wales, Australia
[3] ARC Centre of Excellence for Climate System Science, Monash University, Victoria, Australia

(Manuscript received Nov 2015; accepted Apr 2016)

The Bureau of Meteorology's Australian Water Availability Project (AWAP) daily precipitation analysis provides high resolution rainfall data by interpolating rainfall gauge data, but when evaluated against a spatially dense independent gauge network in the Snowy Mountains large systematic biases are identified. Direct comparisons with the gauge data in May–September between 2007 and 2014 reveal average root mean square errors of about 4.5 mm, which is slightly greater than the average daily precipitation amount, and the errors are larger for higher elevation gauges. A standard Barnes objective analysis is performed on the combined set of independent gauges and Bureau of Meteorology gauges in the region to examine the spatial characteristics of the differences. The largest differences are found on the western (windward) slopes, where the Barnes analysis is up to double the value of the AWAP analysis. These differences are attributed to a) the lack of Bureau of Meteorology gauges in the area to empirically represent the precipitation climatology, and b) the inability of the AWAP analysis to account for the steep topography exposed to the prevailing winds. At high elevation (>1400 m) the Barnes analysis suggests that the precipitation amount is about fifteen percent greater than that of the AWAP analysis, where the difficulties of measuring frozen precipitation likely have a large impact.

1. Introduction

Spatially analysed, or "gridded," rainfall products in mountainous regions are affected by two fundamental problems. Rainfall tends to be more variable in complex terrain, and rain gauge networks are often too sparse or otherwise inadequate to represent this variability. As a result, gridded rainfall datasets tend to underestimate the mean rainfall and smooth out the spatial complexity in mountainous regions. However, mountainous regions are often catchments for important water resources, and the quality of gridded rainfall products affects our ability to accurately predict inflows.

Real-time and historical rainfall spatial analysis began in Australia at the Bureau of Meteorology (BOM) in 1995 when Weymouth et al. (1999) implemented a weighted-average scheme to estimate the precipitation on a regular latitude-longitude grid over the Australian continent. This scheme had some deficiencies (that the authors acknowledge) due to the non-stationary nature of the rain gauge network. In an effort to overcome these deficiencies for the Australian Water Availability Project (AWAP), Jones et al. (2009) implemented an anomaly-based scheme which relied on a gridded rainfall climatology interpolated with splines (described in more detail below), in which a relationship between topographic elevation and seasonal rainfall amount is implicit. A third commonly cited product is the Scientific Information for Land

Corresponding author: Thomas H. Chubb, Lot 3, Pier 8/9 , 23 Hickson Road, Walsh Bay NSW 2000
Email: thomas.chubb@gmail.com

Owners (SILO) (Jeffrey et al., 2001) rainfall analysis, produced by the Queensland government, which uses a combination of interpolating splines and ordinary kriging (e.g. Venkatram, 1988) to interpolate rainfall amounts.

A number of studies have focused on comparisons between the various rainfall analyses. Beesley et al. (2009) compared the error statistics of the AWAP and SILO daily analyses and demonstrated similar performance, with the SILO data performing slightly better in regions of high gauge density. Both analyses had positive biases for low rainfall days and negative biases for high rainfall days. Fawcett et al. (2010) compared the AWAP and BOM analyses in western Tasmania, where the rain gauge density is particularly sparse and many changes have been made over the 20th century, and found that the newer AWAP method substantially addressed the network-induced inhomogeneity of the original BOM analysis. However spurious trends and poor representation of extreme events remain challenges for AWAP in data-sparse regions (King et al., 2013), as it does for any interpolated meteorological product.

Research applications for gridded rainfall analyses vary widely and are too numerous to list exhaustively here. Notably, they have been used to identify and attribute causes to the changes in the spatial patterns of rainfall over the Australian continent (e.g. Timbal and Drosdowsky, 2013; Rotstayn et al., 2012; Gergis et al., 2011), and have informed major projects in climate projections for Tasmania (Grose et al., 2010) and south-eastern Australia (CSIRO, 2010). Another important use of the gridded rainfall products is in rainfall-runoff modelling, in which streamflow estimates are made through closure of the water budget over a river catchment. For example, Chiew et al. (2008) modelled runoff across the Murray-Darling Basin using the SILO analysis and highlighted the importance of mountain catchments for Murray-Darling Basin inflows. Tozer et al. (2012) demonstrated that over a single catchment in South Australia, the sensitivity of hydrological models to typical errors in gridded rainfall products could be very large, particularly for extreme rainfall.

The Snowy Mountains region comprises the highest peaks of the Great Dividing Range and is hydrologically very important to south-eastern Australia as it is the source of the Murray, Murrumbidgee and Snowy river systems. It is also the home of the Snowy Mountains Hydroelectric Scheme, which is a major renewable energy producer. These factors make the measurement and prediction of precipitation a priority for the region, and as such it has received some attention recently. For example, Chubb et al. (2011), Dai et al. (2013), and Theobald et al. (2015) provided different synoptic climatologies for wintertime precipitation in the Snowy Mountains, while Fiddes et al. (2015) and Landvogt et al. (2008) provided similar climatologies for the more general Australian alpine regions. The findings of the various climatologies were somewhat self-evident in that strong dynamic signatures (cut-off lows, cold fronts) and moisture transport were associated with the heaviest precipitation. Several of these studies also noted that the topography of the Great Dividing Range also played an important role, and spatial correlations of daily rainfall amount on the western (windward) slopes tended to be much higher than on the eastern (leeward) slopes.

Measurement of precipitation in the alpine regions of Australia lags international standards. At elevations above 1400 m, precipitation frequently falls as snow in the wintertime, but the tipping-bucket type gauges deployed here are not well-suited to recording frozen precipitation, especially in windy conditions (Chubb et al., 2015), or when frozen precipitation rates greater than about 3 mm/hr overcome the gauge heating capability (Gorman, 2003). Moreover, the BOM rain gauge network is quite sparse in the mountainous areas, which is known to be problematic for the representation of the spatial variability of precipitation. For example, Frei and Schär (1998) performed a climatology of precipitation using a high-resolution gauge network (typical gauge spacing of 10 km) in the European Alps, and found that the precipitation patterns were highly sensitive to the gauge network density. They also noted that no simple altitude/precipitation relationship existed across the European Alps because much of the signal was dominated by topographic slope, aspect, and shielding.

Figure 1. Smoothed south-eastern Australian topography (colours), major rivers and state borders. The Snowy Mountains study region is indicated by the box, which is enlarged in figure 2. In this and subsequent figures, the location of Mt. Kosciusko is shown by a white triangle marker.

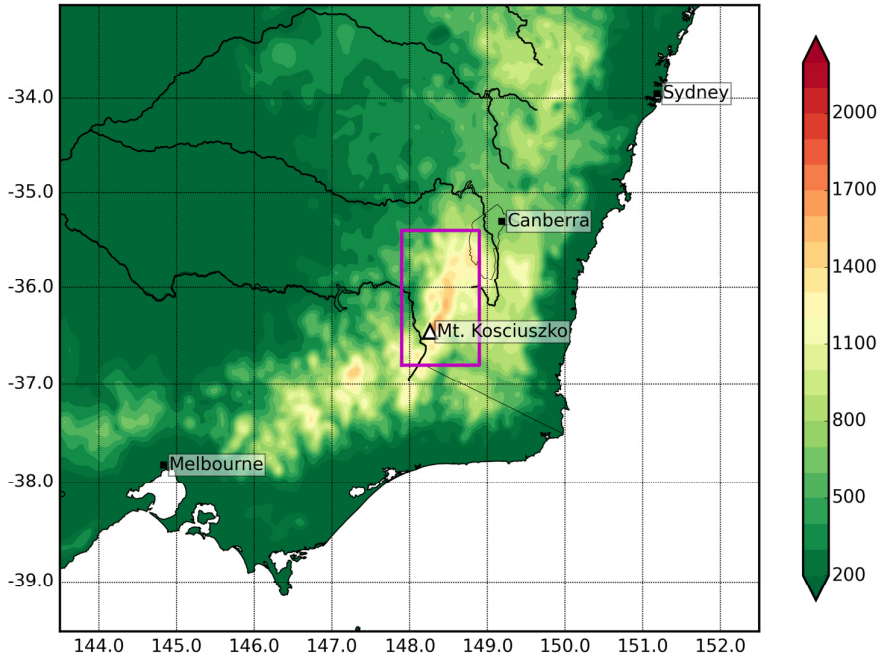

In recent years, a dense, independent network of all-weather precipitation gauges has been deployed in the Snowy Mountains. This provides a unique opportunity to investigate the quality of the AWAP daily rainfall analyses in the challenging environment of the Snowy Mountains. We will present comparisons between a) the AWAP analysis and the independent gauges, and b) the AWAP analysis and a simple optimised Barnes analysis of all rain gauges in the region.

2. Analysis region, precipitation data and methods

2.1 The Snowy Mountains region and analysis periods

The Snowy Mountains comprise the highest peaks on the Australian continent and are approximately mid-way between Melbourne and Sydney on the Great Dividing Range (figure 1). An ongoing weather modification project (Manton et al., 2011) necessitated the installation of an enhanced precipitation gauge network in the mountains, which is described in more detail below. This paper focuses on precipitation observations between May and September (when the gauge network is fully deployed) during the years of 2007–2014 inclusive. For this paper, we defined an analysis region of 1° longitude by 1.5° latitude centred on the Snowy Mountains (147.9–148.9°E, 35.4–36.9°S).

2.2 Bureau of Meteorology gauges and spatial analysis

The Australian Bureau of Meteorology (BOM) operates a national weather station network incorporating a variety of different precipitation gauge types. The most commonly used in the Snowy Mountains region are the standard 203 mm non-recording gauge for daily (manual) precipitation measurements, and Rimco model 7499 and 8020 tipping bucket gauges at Automatic Weather Station (AWS) locations. The quality-controlled daily precipitation data are available for download from the BOM website, and for this paper we obtained data from all gauges within the analysis region and in a 0.3° buffer surrounding it. Especially for manual gauges, the BOM gauge data includes accumulated amounts over several days, but these were excluded from our analysis. Following this, a total of 38 BOM gauges were operational in the analysis region, with a further 73 in the buffer region, for at least one day during the analysis period (figure 2a; note that the buffer region is not entirely shown). It is immediately apparent that the density of the BOM gauge network is low in the mountainous

regions, with only five high elevation (>1400 m) gauges located at the major ski resorts, in the alpine town of Cabramurra, and on Mt Ginini to in the north east of the analysis region.

Figure 2. Detail of analysis region, with topographic elevation (metres) in colours, and locations of Australian Bureau of Meteorology (BOM) gauges (a) and Snowy Hydro Limited (SHL) gauges (b). The grey symbols in (b) indicate gauges that were installed during the analysis period, mostly in 2009. Note that some gauges (both BOM and SHL) used in the analysis were located outside the regions shown.

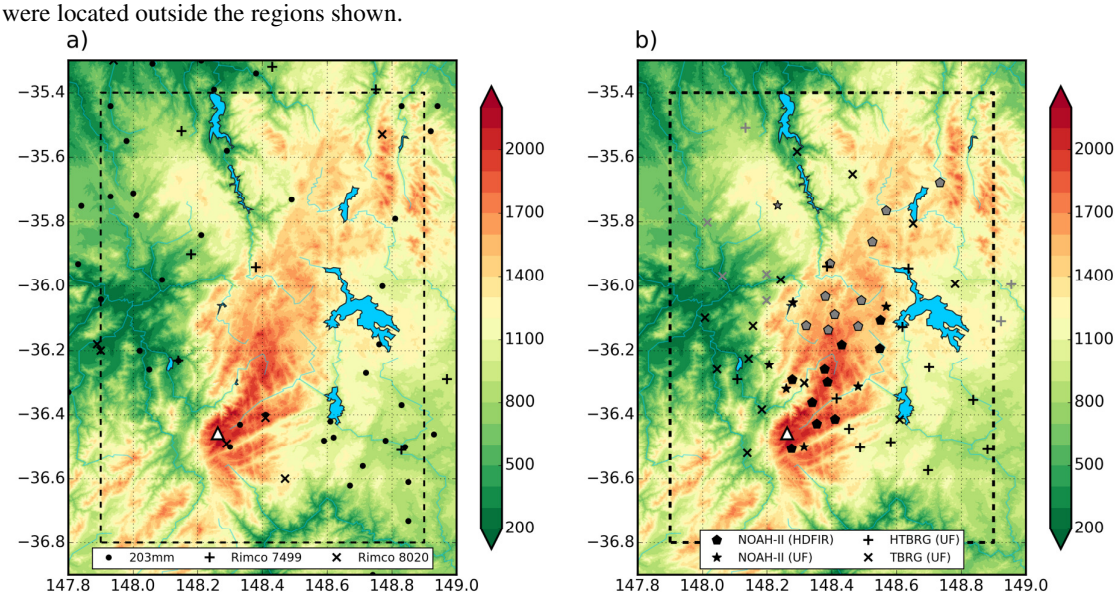

Jones et al. (2009) describe a spatial analysis technique used by the BOM to interpolate rainfall observations on to a 0.05° ×0.05° grid. The approach requires the calculation of a gridded 30 year climatology for each month. This is interpolated from the weather station data using tri-variate thin plate interpolating splines (Wahba and Wendelberger, 1980), which directly incorporate a long-term relationship between topographic elevation and rainfall. This methodology has a demonstrated advantage over both simple two-dimensional interpolation schemes and those that use a linear dependence on elevation (Hutchinson, 1995). The daily and monthly station observations are then expressed as multiplicative anomalies with respect to the climatology, and a Barnes successive correction scheme (Koch et al., 1983) is used to calculate a spatial analysis of the anomalies. The gridded anomalies are then multiplied by the gridded climatology to produce the rainfall spatial analysis. The analyses are available in near real-time, but are continually reprocessed as the manual observational data may take some time to become available. Similar techniques are used for temperature, water vapour pressure, and solar radiation, except that the anomalies are expressed in absolute terms. The analyses are publicly available on the BOM website (www.bom.gov.au/jsp/awap).

Cross-validation of the AWAP rainfall analyses, performed with a bootstrap method in which five percent of the data were removed at a time, was also presented by (Jones et al., 2009). The national average root mean square error (RMSE) for the period 2001–2007 was given as 3.1 mm for daily precipitation. The daily error fields on the same spatial grids as the rainfall analyses are also available for download and are used in this paper.

2.3 Snowy Hydro precipitation gauge data

Snowy Hydro Ltd (SHL), the operator of the Snowy Mountains Hydroelectric Scheme, has maintained a network of precipitation gauges in the region since the 1950s (figure 2b). Historically, these have been used for hydrological purposes, and indeed some have been incorporated into the current BOM network, but since 2005 many additional gauges have been installed to evaluate the Snowy Precipitation Enhancement Research Project (SPERP) (Manton et al., 2011). At high elevations, where snow is frequently reported, ETI Noah-II all-weather precipitation gauges (ETI Instrument Systems Inc., 2008) were installed, and a mixture of heated and unheated tipping bucket gauges were installed at lower elevations. There were a total of 77 gauges at 66 unique sites during the analysis period, with a maximum of 74 operational in any single year (see figure 3). Rain gauge data were quality controlled by SHL technicians and archived on 30 minute intervals.

Figure 3. Number of SHL precipitation gauges deployed in Snowy Mountains region that were deployed on 1 October of each year. The solid lines represent the total number of each gauge type for each year, and the dashed lines represent the number of those that were above 1000m ASL. "UF" indicates NOAH-II gauges that were unfenced (but had Alter shields), and HDFIR indicates NOAH-II gauges in a double wind fence.

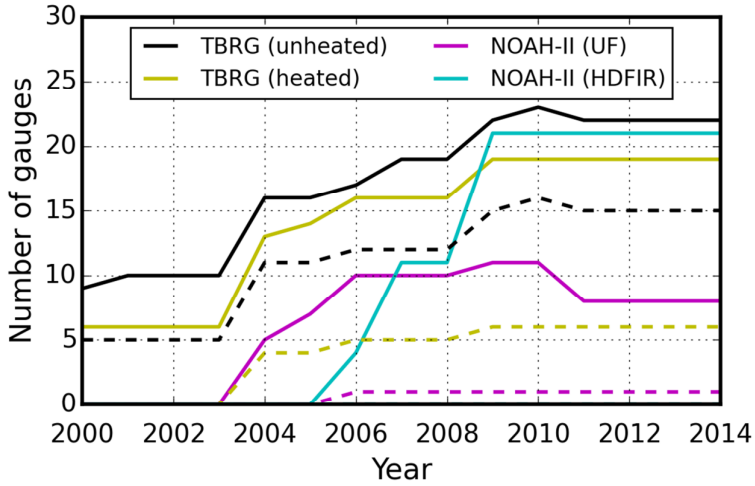

All of the gauges installed for the SPERP had a degree of protection from the wind, ranging from manufacturer-specified (Alter, 1937) shields, to custom-made double wind-fences similar to those used in the World Meteorological Organisation Solid Precipitation Measurement Intercomparison (Goodison et al., 1998), at particularly exposed locations. In particular, a large number of new Noah-II gauges with double fences were installed in 2009 to accommodate the expansion of the SPERP. Some of these were at existing Noah-II sites with no wind fences, and in most cases the unfenced gauges were removed after a year or so.

Chubb et al. (2015) evaluated the impact of the double fences on the catch efficiency of the Noah-II gauges, and found that a fenced gauge could record as much as 50 percent more precipitation in certain conditions at the most exposed locations in the Snowy Mountains. A more realistic seasonal value for this "under-catch" is probably around 15 percent, as was recorded at a site at 1586 m elevation, where 33 percent of the total precipitation was identified as either snow or mixed-phase precipitation. Those authors suggested an adjustment scheme, based on regression analysis of gauge efficiency with respect to wind speed and temperature for different precipitation categories, to account for the difference in precipitation reported by Analysis region, precipitation data and methods

2.4 Estimating seasonal average rainfall from gauge data

Most of the gauges had some missing data which affected the calculation of seasonal average rainfall. To account for the underestimate due to missing data, we gap-filled the gauge data using linear regression to the nearest AWAP gridpoint. We required that at least 80 percent of the gauge data be available over the 8 year to calculate the seasonal averages. This approach estimate assumes that the gaps are randomly distributed through the time series and that the relationships between the AWAP analysis and the gauge amounts are stationary. Neither of these assumptions is likely to be strictly valid, so we do not use these estimates for anything other than illustrative purposes.

2.5 Spatial analysis of precipitation gauge data

To assess the spatial variability of precipitation represented in the AWAP analysis, we performed a simple spatial analysis of the combined SHL and BOM gauge data. Between 150 and 170 gauges contributed at least one day to the analysis in each year. We applied a Barnes successive-correction method directly to the precipitation amount rather than to the anomalies as for the AWAP analysis. This approach assumes that the density of the gauge network is sufficient to represent the variability due to the topography and doesn't require a robust baseline climatology. We began by defining an initial guess $P_{g,0}$ for each grid point as follows:

Figure 4. (a) Mean AWAP May-September total precipitation (from gridded daily totals) for 2007–2014, with estimates of total SHL gauge amounts (requiring at least 80 percent of the data to be available) shown by markers. (b) Root mean squared AWAP error estimate field, with RMSE with respect to SHL gauges shown by markers. Also shown are terrain contours with 200 m interval and the 1000 m contour in heavier weight, and the major river catchment boundaries are shown by dot-dash lines and annotated in (a).

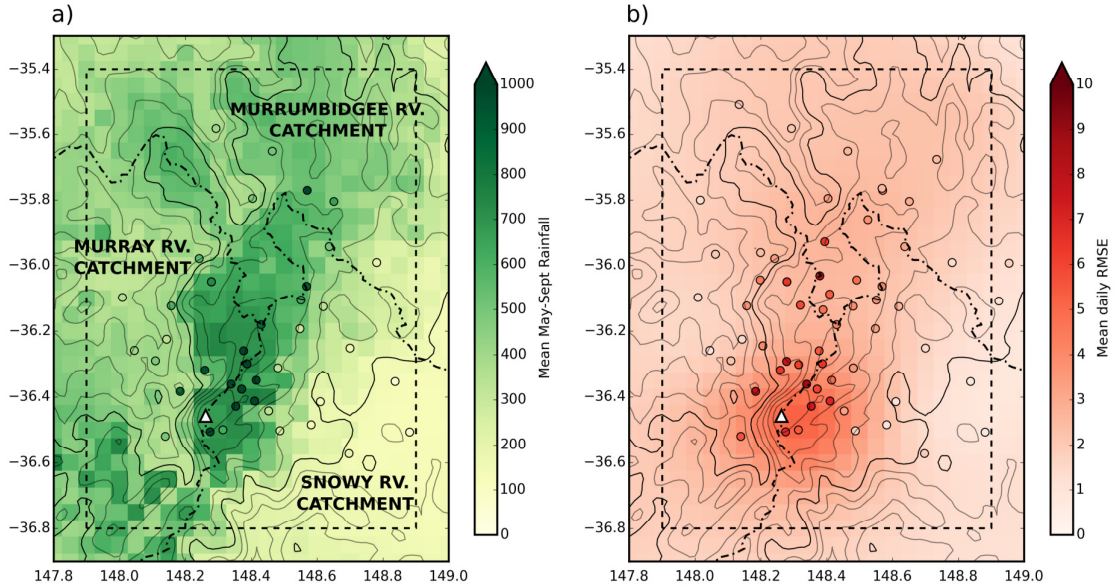

$$P_{g,0} = \frac{\sum w_n P_n}{\sum w_n}$$

where P_n are the station observations, and the weights applied to each station datum are defined by $w_n = \exp(-d_n^2/4c)$, where d_n are the distances from the stations to the grid point, and c is a parameter which controls the fall-off of the weight with distance from the station. Successive iterations are calculated by interpolating the previous gridded values back to the station locations using cubic splines to give the set of values $P_{g,k-1}(n)$ and applying a correction to the first guess:

$$P_{g,k} = P_{g,k-1} + \frac{\sum w_n' \left[P_n - P_{g,k-1}(n)\right]}{\sum w_n'}$$

where the new weights are defined as $w_n' = \exp(-d_n^2/4gc)$, with the additional parameter $0 < g \leq 1$ defining a steeper fall-off with distance for smaller values of g. We applied a trimming method on the final output to ensure that each grid point was influenced by at least three stations that were within six grid lengths (about 30 km); grid points that were not were set to a missing value.

Rules of thumb exist for c and g. A typical first guess for the value of c is given by $c=A/N$, where A is the area of the analysis region (degrees squared) and N is the number of observational sites, so a value of c=0.01 would be consistent for our situation. The value of g is typically set to 0.5 for the second and subsequent passes. We performed a test to determine optimal parameters through a bootstrap method. One site was removed from the combined gauge dataset and the spatial analysis was performed with the remaining gauges for 90 pairs of c and g, and the output from the nearest gridpoint to the deleted gauge retained. This was repeated for each of the gauges to permit an overall RMSE calculation using a statistically independent dataset for each parameter pair.

Figure 5. Number of SHL gauges above a given height (magenta; left axis) and overall daily RMSE (cyan; right axis) of the AWAP analysis compared against those gauges. The mean precipitation amount per day for the same gauges is shown by the yellow line.

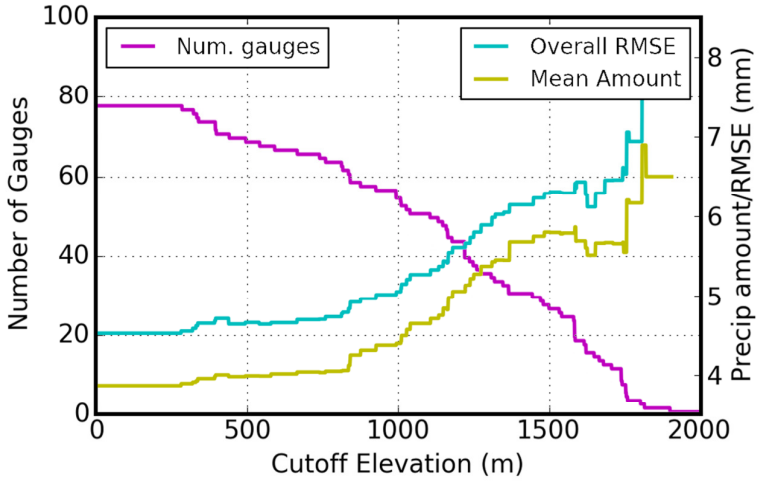

We found that a three-pass scheme (i.e. two iterations after the initial guess) produced slightly better results than a two-pass scheme, which is consistent with other studies (Achtemeier, 1987; Barnes, 1994a; Weymouth et al., 1999). The available literature suggests that there is not much to be gained by the use of a four-pass scheme (Barnes, 1994b) and we have not considered them for this paper. The optimal values of c and g from this analysis were found to be 0.01 and 0.6 respectively, which produced an RMSE of 2.712 mm. There was low sensitivity to the value of g, with a value of 0.5 resulting in an RMSE of 2.714 mm. This bootstrap optimisation has the advantage of providing the cross-validation statistics for the spatial analysis, which we compare to the values obtained for the AWAP analysis below.

3. Accuracy of the AWAP rainfall analysis in the Snowy Mountains

Figure 4a shows the mean May–September total precipitation distribution in the analysis region for the gridded AWAP product and the estimated value for the SHL gauges. Precipitation amount is highly correlated with topography, with the highest amounts falling along the crest of the mountains in both datasets. The rain shadow effect over the Monaro Plains (lower right corner) is also clearly evident in both datasets. Lower lying areas to the west of the main range typically receive 300–500 mm in this season, whereas in the Monaro Plains precipitation amounts of 100 mm are more common.

There is a systematic bias in the precipitation amounts from the two data sources. The highest seasonal value in the AWAP analysis was 775 mm, but many of the SHL gauges reported in excess of 1000 mm, which is more consistent with the longer-term values presented by Chubb et al. (2011) for the same season and region. These discrepancies are in excess of the catch ratio corrections suggested by Chubb et al. (2015), but could at least in part be attributed to poor performance of tipping bucket gauges in alpine conditions. There is a spatial pattern to the bias, with some gauges on the western slopes of the mountains recording considerably more than the analysis amount, and conversely several gauges on the eastern slopes reported less than the analysis. We investigate these patterns through the use of the Barnes spatial analysis below.

Table 1. Root mean square error of the gridded precipitation fields derived either by bootstrap method or direct comparison with independent data.

	Bootstrap validation RMSE (mm)		*Direct validation RMSE (mm)*	
	Mean	Max	Mean	Max
AWAP	2.25	5.2	4.5	8.9
Barnes	2.71	6.1	-	-

Figure 6. Quantile-quantile plots of gauge daily precipitation amounts vs. AWAP nearest gridpoint daily precipitation amounts. Note logarithmic scale and truncation at 0.1mm.

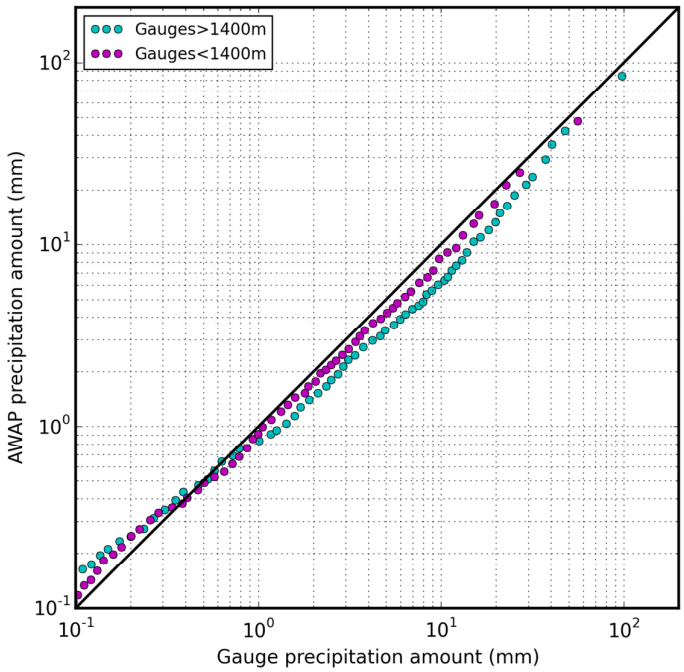

The AWAP analysis RMSE in figure 4b (and table 1) was derived by averaging the square of the daily RMSE fields that were produced through the bootstrap analysis by the BOM, and taking the square root of the result. The mean value across the analysis region was 2.25 mm, and there was an increase to 5.2 mm near Mt. Kosciuszko. However, when the RMSE was calculated by comparing the independent SHL gauges against their nearest gridpoints in the AWAP analysis much larger values were obtained. The overall value for all gauges with greater than 50 percent of the daily data available was 4.5 mm, the maximum value was 8.9 mm, and for gauges above 1400 m ASL (22 gauges), the overall value was 6.1 mm (see table 1).

When the RMSE values were stratified by gauge elevation a nearly monotonic relationship was revealed (figure 5), but this can largely be explained by the increase in precipitation with topographic elevation. However we note that, on average, the mean RMSE was greater than the mean daily precipitation amount, and this was also the case on average when the gauges were stratified by elevation.

Figure 6 shows the quantile-quantile plot for daily average precipitation amount over all available gauges and their nearest gridpoint in the AWAP analysis. As found in an assessment of the national AWAP and SILO analyses by Beesley et al. (2009), the biases with respect to the gauge data were different for different rainfall amounts. For dry days, on which the mean rainfall amount was less than about 0.5 mm, the AWAP analysis tended to have a positive bias, whereas on wet days the bias was negative. Care must be taken, however, when interpreting the very low precipitation amounts where the daily rainfall amount value is close to the resolution of the gauges (0.2 mm for most of the gauges) due to quantisation artefacts in the averaging. The negative bias appears to be exacerbated for the higher elevation gauges, where the peak bias for gauge mean amounts of about 10 mm corresponded to AWAP nearest gridpoint values of only 6 mm. Interestingly, the relative bias was reduced for higher precipitation amounts. This is consistent with Chubb et al. (2015), who found that undercatch was reduced for higher precipitation rates (other factors being equal). It may also reflect the tendency for very heavy precipitation to be in the form of rain rather than snow, making the precipitation measurement less affected by wind speed (Chubb et al., 2015).

Figure 7. Barnes analysis for all precipitation gauges and cross-validated RMSE. Terrain contours and catchment boundaries are shown as previously. Gauge locations are shown with open markers. Annotation "X" marks the head of the Tumut River valley, discussed in text.

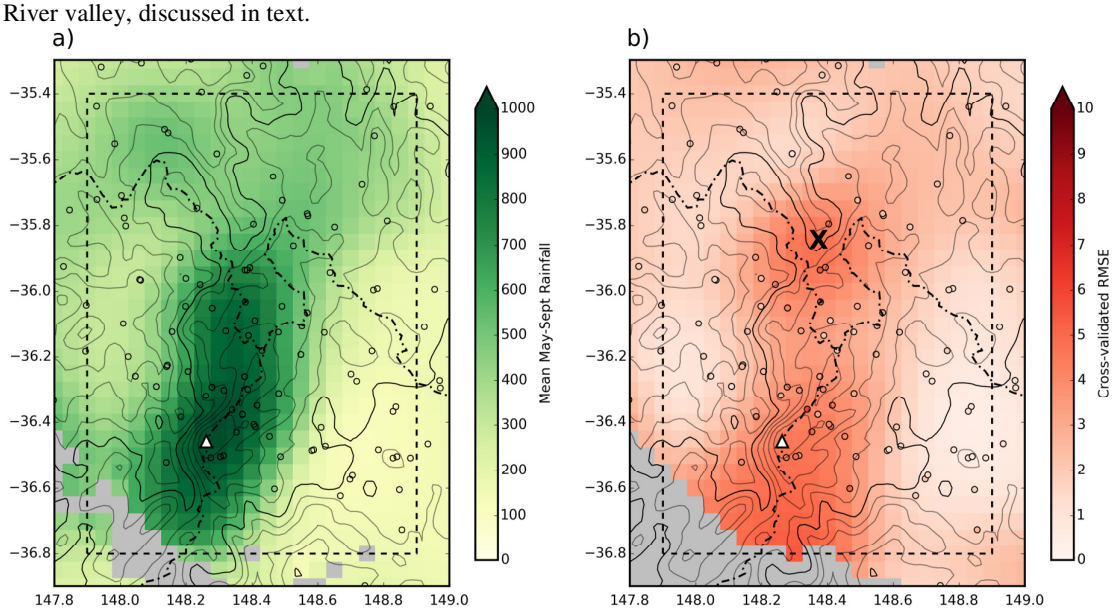

4. Barnes spatial analysis of gauge data

Figure 7a shows the spatial distribution of the mean May-September precipitation amount derived using the Barnes analysis procedure described above and gauge data from both the BOM and SHL. The missing values represent grid cells for which there were insufficient local data (at least three gauges within 0.3° range) on one or more days during the entire analysis period.

The minimised RMSE from the bootstrap parameter optimisation (which serves as a full cross-validation) is shown in figure 7b, with the values for individual sites shown by the markers (see also table 1). The RMSE was also interpolated with a Barnes analysis and is shown by the colours. Unsurprisingly, the RMSE is highest over the mountains (typically 4–5 mm) because it tends to scale with the precipitation amount, which is highest there. It is highest to the south of the Snowy Mountains where the gauge network is quite sparse. There is a secondary maximum at the head of the Tumut River gorge (annotated by X in figure 7b), which is an area of especially complex terrain.

The difference between the Barnes analysis and the AWAP analysis over the analysis period is shown in figure 8, which has some interesting features that are discussed in more detail below. The mean May–September precipitation amount over the region depicted was 456 mm for the Barnes analysis and 421 mm for the AWAP analysis; a difference of 7.8 percent, but the biggest differences between the analyses are clearly in the vicinity of the main range.

Figure 8. Difference between Barnes analysis and the AWAP analysis (colours; mm) for mean May–September precipitation. The contiguous region in the Snowy Mountains above 1400 m is hatched. Here the SHL gauge locations are shown with open markers and the BOM gauge locations are shown by crosses. The annotations A-F are discussed in text.

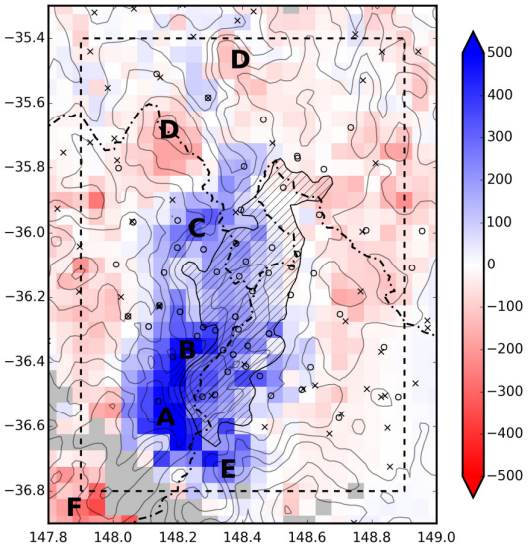

5. Discussion

5.1 Robustness of the Barnes analysis

We performed a spatial analysis of the combined BOM/SHL gauge network analysis using the gauge data alone, without accounting for the climatological impact of topographical elevation. A bootstrap cross-validation of the analysis produced similar RMSE statistics to those published for the AWAP analysis, although we showed separately that the AWAP RMSE statistics are underestimated in the Snowy Mountains. . We used the simple Barnes analysis to highlight the spatial patterns in the discrepancies between the gauge data and the AWAP analysis, while recognising that superior analysis techniques could provide even more accurate results.

Our Barnes analysis suggests that rather more precipitation occurs on the western slopes of the Snowy Mountains around Tom Groggin and Geehi (the areas marked by “A” and “B” in figure 8 and discussed further below) than is represented in the AWAP analysis. The BOM has no gauges in this area and relies exclusively on interpolation of anomalies from reasonably distant locations, but there were several SHL gauges explicitly informing our Barnes analysis. Differences were also large in the Jagumba region (“C”) at elevations of about 1000 m, and several gauges informed the analysis here so we regard the spatial analysis as robust.

Differences between the two fields also occur in the complex terrain around the Tumut River gorge (marked “D-D”). There is high terrain on either side of the gorge that is relatively sparse of gauges, and the AWAP analysis shows a greater precipitation amount here, as it does for a handful of other small prominences where there are no gauges. On the other hand, the differences in the Pilot Wilderness (“E”) were not informed by nearby gauges and we do not consider these to be as robust. Likewise, the area in the south-western corner (“F”) is only informed by some relatively distant BOM gauges and we disregard the differences there.

As discussed above, there were changes to the SHL gauge network over the analysis period, in particular between September 2008 and May 2009. As Fawcett et al. (2010) point out, this opens the possibility of network induced inhomogeneities in the Barnes analysis that we used to compare against the AWAP analysis. The dataset prior to the majority of the changes is not long enough to assess this statistically, but we have repeated each of the analyses for the period 2009–2015, during which the gauge network was relatively stationary, and our conclusions were not significantly affected.

We also took the precaution of repeating all analyses with the raw gauge data, instead of the data homogenised according to the recommendations of Chubb et al. (2015). The difference between the "adjusted" and "raw" analyses was 0.57 percent over the entire region, and for points above 1400 m it was 1.09 percent, so the impact on the comparisons with the AWAP analysis was negligible.

5.2 Differences between the analyses

Around Tom Groggin and Geehi (the areas marked by "A" and "B"), differences between the seasonal precipitation amounts exceed 400 mm, which is roughly equivalent to the amounts for the AWAP analysis. The terrain elevation is not especially high, between 600 and 1200 m, but it is rather steep, with mean gradients in some areas above twenty percent. The topographical gradient (in terms of "mountain width") and aspect have been shown in many theoretical studies to have strong influence on rainfall amounts (Colle, 2004; Jiang, 2003; Watson and Lane, 2014), and it has been long understood that there are differences between the precipitation patterns on upwind and downwind mountain slopes (e.g. Smith, 1979; Frei and Schär, 1998). In the Snowy Mountains, the steepest slopes are directly exposed to the prevailing westerly winds, so it should be expected that the precipitation amount would be disproportionate to the topographic elevation. Indeed, Chubb et al. (2015) showed that the heaviest precipitation in the Snowy Mountains was associated with back trajectories perpendicular to the gradient of the mountains, and as a side note, Chubb et al. (2012) considered some case studies of wintertime storms in the Brindabella ranges (which are in the north-east of the analysis region) and found distinctly higher radar average reflectivity on the upwind side of the ranges.

The methodology of the AWAP analysis relies on a gridded climatology, which is essentially a three-dimensional interpolation from the station data and includes no information about terrain gradient. This approach directly accounts for the effect of topographic elevation on seasonal precipitation amounts, which is why the AWAP analysis suggests more precipitation around the some of the smaller prominences in figure 8 as discussed above. Accounting for the exposure of steep terrain to high winds is harder, but has been performed in other national precipitation analyses (e.g. Daly et al., 1994) As an alternative, the inclusion of the SHL gauges presented in this paper to modify the climatological values on the western slopes of the Snowy Mountains could have some merit. However, the AWAP analysis for the exposed slopes of other mountains along the Great Dividing Range is likely to have similar deficiencies and there are no other high-quality independent gauge networks available to either characterise or rectify these.

"Alpine" precipitation was systematically under-represented by the AWAP analysis. Within the closed 1400 m contour (hatched in figure 8) the mean amount from the Barnes analysis was 778 mm, compared to 648 mm in the AWAP analysis, a difference of about 16.7 percent. The spatial analysis of alpine precipitation faces the additional challenge of large uncertainties in the gauge observations. At the BOM Thredbo AWS, which has a tipping bucket gauge installed, the conditions are very exposed with mean 3pm winds in July of 9.0 ms-1. Chubb et al. (2015) showed that similar gauges in the Snowy Mountains could be expected to report about half of the snow (compared to well-protected Noah-II gauges) for winds of this magnitude, and over the course of a winter season the accumulated deficit could be 15-50 percent. This factor alone could account for the difference in the analyses at high elevations.

The differences between the analyses may be expressed on a per catchment basis (see annotations in Figure 4a). The Murray River catchment received an estimated 18 percent less precipitation in the AWAP analyses than in the Barnes, and the Snowy River catchment received an estimated 9 percent less. Expressed in volumes, this equates to 419 and 146 GL respectively, which is comparable to the total annual releases to the Murray-Darling Basin from the Snowy Mountains Scheme (Murray-Darling Basin Authority, 2013). Obviously hydrological modelling would need to be undertaken to convert these values to streamflows, but the importance of resolving these differences is unequivocal.

6. Conclusions

We have presented an evaluation of the May–September AWAP gridded daily precipitation analyses over the Snowy Mountains region of south-eastern Australia using data from a fully independent gauge network (SHL gauges only). The complexity of the terrain, the sparseness of the BOM gauge network in this region, and the difficulties associated with measuring frozen precipitation makes it something of a worst-case scenario for precipitation spatial analysis. Using the gauge data alone, it was shown that the daily error estimates from the AWAP objective analysis scheme, which had maximum values of about 2.6 mm, were too small. The mean RMSE over all gauges from our analysis was about 4.5 mm, and

for gauges above 1400 mm it was greater than 6.0 mm. In fact, the RMSE was in general greater than the mean daily precipitation amount.

We applied a simple three-pass Barnes successive-correction scheme to examine the spatial patterns in the differences between the combined BOM and SHL gauge networks and the AWAP analysis. The largest biases were found on the steep western slopes of the mountains which are commonly exposed to the prevailing winds. This topographical complexity is not accounted for in either of the spatial analysis methodologies. However, the Barnes analysis, with access to more gauge data, was better able to capture the topographically induced variability, which may be the reason for the differences here. The differences between the two analyses are also large in the alpine areas above 1400 m, where the measurement of frozen precipitation is especially important. Improving the spatial representation of precipitation in these areas has the potential to substantially improve hydrological modelling for streamflows.

Acknowledgements

The authors would like to acknowledge funding from an ARC linkage grant (LP120100115).

References

Achtemeier, G.L. 1987. On the Concept of Varying Influence Radii for a Successive Corrections Objective Analysis. *Mon. Weather Rev.* 115, 1760–1772.

Alter, J.C. 1937. Shielded storage precipitation gages. *Mon. Weather Rev.* 65, 262–265.

Barnes, S.L. 1994a. Applications of the Barnes Objective Analysis Scheme. Part II: Improving Derivative Estimates. *J. Atmospheric Ocean. Technol.* 11, 1449–1458.

Barnes, S.L. 1994b. Applications of the Barnes Objective Analysis Scheme. Part III: Tuning for Minimum Error. *J. Atmospheric Ocean. Technol.* 11, 1459–1479.

Beesley, C.A., Frost, A.J. and Zajaczkowski, J. 2009. A comparison of the BAWAP and SILO spatially interpolated daily rainfall datasets. Presented at the 18th World IMACS/MODSIM Congress, Cairns, Australia, pp. 3886–3892.

Chiew, F., Vaze, J., Viney, N., Jordan, P., Perraud, J.-M., Zang, L., Teng, J., Arancibia, J.P., Morden, R., Freebairn, A., Austin, J., Hill, P., Wiesemfeld, C. and Murphy, R. 2008. Rainfall-runoff modelling across the Murray-Darling Basin, A report to the Australian Government from the CSIRO Murray-Darling Basin Sustainable Yields Project, Water for a Healthy Country Flagship. CSIRO, Australia.

Chubb, T.H., Manton, M.J., Siems, S.T., Peace, A.D. and Bilish, S.P. 2015. Estimation of wind-induced losses from a precipitation gauge network in the Australian Snowy Mountains. *J. Hydrometeorol.* doi:10.1175/JHM-D-14-0216.1

Chubb, T.H., Morrison, A.E., Caine, S., Siems, S.T. and Manton, M.J. 2012. Case studies of orographic precipitation in the Brindabella Ranges: model evaluation and prospects for cloud seeding. *Aust. Meteorol. Oceanogr. J.* 62, 305–321.

Chubb, T.H., Siems, S.T. and Manton, M.J. 2011. On the Decline of Wintertime Precipitation in the Snowy Mountains of Southeastern Australia. *J. Hydrometeorol.* 12, 1483–1497. doi:10.1175/JHM-D-10-05021.1

Colle, B.A. 2004. Sensitivity of Orographic Precipitation to Changing Ambient Conditions and Terrain Geometries: An Idealized Modeling Perspective. *J. Atmospheric Sci.* 61, 588–606.

CSIRO, 2010. Climate variability and change in south-eastern Australia: A synthesis of findings from Phase 1 of the South Eastern Australian Climate Initiative (SEACI). Commonwealth Scientific and Industrial Research Organisation (CSIRO Australia).

Dai, J., Manton, M.J., Siems, S.T. and Ebert, E.E. 2013. Estimation of Daily Winter Precipitation in the Snowy Mountains of Southeastern Australia. *J. Hydrometeorol.* 15, 909–920. doi:10.1175/JHM-D-13-081.1

Daly, C., Neilson, R.P. and Phillips, D.L. 1994. A Statistical-Topographic Model for Mapping Climatological Precipitation over Mountainous Terrain. *J. Appl. Meteorol.* 33, 140–158.

ETI Instrument Systems Inc. 2008. NOAH-II (TM) Total Precipitation Gauge (12-inch Capacity Manually Serviced) Technical Manual. ETI Instrument Systems Inc.

Fawcett, R., Trewin, B. and Barnes-Keoghan, I. 2010. Network-derived inhomogeneity in monthly rainfall analyses over western Tasmania. *IOP Conf. Ser. Earth Environ. Sci.* 11, 012006. doi:10.1088/1755-1315/11/1/012006

Fiddes, S.L., Pezza, A.B. and Barras, V. 2015. Synoptic climatology of extreme precipitation in alpine Australia. *Int. J. Climatol.* 35, 172–188. doi:10.1002/joc.3970

Frei, C. and Schär, C. 1998. A precipitation climatology of the Alps from high-resolution rain-gauge observations. *Int. J. Climatol.* 18, 873–900.

Gergis, J., Gallant, A.J.E., Braganza, K., Karoly, D.J., Allen, K., Cullen, L., D'Arrigo, R., Goodwin, I., Grierson, P. and McGregor, S. 2011. On the long-term context of the 1997–2009 "Big Dry" in South-Eastern Australia: insights from a 206-year multi-proxy rainfall reconstruction. *Clim. Change* 111, 923–944. doi:10.1007/s10584-011-0263-x

Goodison, B.E., Louie, P.Y. and Yang, D. 1998. WMO Solid Precipitation Measurement Intercomparison.

Gorman, J.D. 2003. Laboratory Evaluation Of The Bureau Designed Heated Tipping Bucket Rain Gauge (Instrument Test Report No. ITR675). Bureau of Meteorology.

Grose, M.R., Barnes-Keoghan, I., Corney, S.P., White, C.J., Holz, G.K., Bennett, J.B., Gaynor, S.M. and Bindoff, N.L. 2010. General Climate Impacts, Climate Futures for Tasmania. Antarctic Climate and Ecosystems Cooperatice Research Centre, Hobart, Tasmania.

Hutchinson, M.F. 1995. Interpolating mean rainfall using thin plate smoothing splines. *Int. J. Geogr. Inf. Syst.* 9, 385–403. doi:10.1080/02693799508902045

Jeffrey, S.J., Carter, J.O., Moodie, K.B. and Beswick, A.R. 2001. Using spatial interpolation to construct a comprehensive archive of Australian climate data. *Environ. Model. Softw.* 16, 309–330. doi:10.1016/S1364-8152(01)00008-1

Jiang, Q. 2003. Moist dynamics and orographic precipitation. *Tellus A* 55, 301–316. doi:10.1034/j.1600-0870.2003.00025.x

Jones, D.A., Wang, W. and Fawcett, R. 2009. High-quality spatial climate data-sets for Australia. *Aust. Meteorol. Oceanogr. J.* 58, 233–248.

King, A.D., Alexander, L.V. and Donat, M.G. 2013. The efficacy of using gridded data to examine extreme rainfall characteristics: a case study for Australia. *Int. J. Climatol.* 33, 2376–2387. doi:10.1002/joc.3588

Koch, S.E., desJardins, M. and Kocin, P.J. 1983. An Interactive Barnes Objective Map Analysis Scheme for Use with Satellite and Conventional Data. *J. Clim. Appl. Meteorol.* 22, 1487–1503.

Landvogt, P.K., Bye, J.A.T. and Lane, T.P. 2008. An investigation of recent orographic precipitation events in northeast Victoria. *Aust. Meteorol. Mag.* 57, 235–247.

Manton, M.J., Warren, L., Kenyon, S.L., Peace, A.D., Bilish, S.P. and Kemsley, K. 2011. A Confirmatory Snowfall Enhancement Project in the Snowy Mountains of Australia. Part I: Project Design and Response Variables. *J. Appl. Meteorol. Climatol.* 50, 1432–1447. doi:10.1175/2011JAMC2659.1

Murray-Darling Basin Authority, 2013. Surface water in the Basin [WWW Document]. URL http://www.mdba.gov.au/what-we-do/water-planning/surface-water-in-the-basin (accessed 10.8.15).

Rotstayn, L.D., Jeffrey, S.J., Collier, M.A., Dravitzki, S.M., Hirst, A.C., Syktus, J.I. and Wong, K.K. 2012. Aerosol- and greenhouse gas-induced changes in summer rainfall and circulation in the Australasian region: a study using single-forcing climate simulations. *Atmospheric Chem. Phys.* 12, 6377–6404. doi:10.5194/acp-12-6377-2012

Smith, R.B. 1979. The influence of mountains on the atmosphere, in: Advances in Geophysics. Academic Press, pp. 87–230.

Theobald, A., McGowan, H., Speirs, J. and Callow, N. 2015. A Synoptic Classification of Inflow-Generating Precipitation in the Snowy Mountains, Australia. *J. Appl. Meteorol. Climatol.* 54, 1713–1732. doi:10.1175/JAMC-D-14-0278.1

Timbal, B., Drosdowsky, W. 2013. The relationship between the decline of Southeastern Australian rainfall and the strengthening of the subtropical ridge. *Int. J. Climatol.* 33, 1021–1034. doi:10.1002/joc.3492

Tozer, C.R., Kiem, A.S. and Verdon-Kidd, D.C. 2012. On the uncertainties associated with using gridded rainfall data as a proxy for observed. *Hydrol. Earth Syst. Sci.* 16, 1481–1499. doi:10.5194/hess-16-1481-2012

Venkatram, A. 1988. On the use of kriging in the spatial analysis of acid precipitation data. *Atmospheric Environ.* 1967 22, 1963–1975. doi:10.1016/0004-6981(88)90086-8

Wahba, G. and Wendelberger, J. 1980. Some New Mathematical Methods for Variational Objective Analysis Using Splines and Cross Validation. *Mon. Weather Rev.* 108, 1122–1143.

Watson, C.D. and Lane, T.P. 2014. Further Sensitivities of Orographic Precipitation to Terrain Geometry in Idealized Simulations. *J. Atmospheric Sci.* 71, 3068–3089. doi:10.1175/JAS-D-13-0318.1

Weymouth, G., Mills, G.A., Jones, D., Ebert, E.E. and Manton, M.J. 1999. A continental-scale daily rainfall analysis system. *Aust. Meteorol. Mag.* 48, 169–179.